© 2017. Published by The Company of Biologists Ltd | Journal of Experimental Biology (2017) 220, 3336-3343 doi:10.1242/jeb.157941

RESEARCH ARTICLE

Regional variation in undulatory kinematics of two hammerhead species: the bonnethead (*Sphyrna tiburo*) and the scalloped hammerhead (*Sphyrna lewini*)

Sarah L. Hoffmann[1,*], Steven M. Warren[2] and Marianne E. Porter[1]

ABSTRACT

Hammerhead sharks (Sphyrnidae) exhibit a large amount of morphological variation within the family, making them the focus of many studies. The size of the laterally expanded head, or cephalofoil, is inversely correlated with pectoral fin area. The inverse relationship between cephalofoil and pectoral fin size in this family suggests that they might serve a complementary role in lift generation. The cephalofoil is also hypothesized to increase olfaction, electroreception and vision; however, little is known about how morphological variation impacts post-cranial swimming kinematics. Previous studies demonstrate that the bonnethead and scalloped hammerhead have significantly different yaw amplitude, and we hypothesized that these species utilize varied frequency and amplitude of undulation along the body. We analyzed video of free-swimming sharks to examine kinematics and 2D morphological variables of the bonnethead and scalloped hammerhead. We also examined the second moment of area along the length of the body and over a size range of animals to determine whether there were shape differences along the body of these species and whether those changed over ontogeny. We found that both species swim with the same standardized velocity and Strouhal number, but there was no correlation between two-dimensional morphology and swimming kinematics. However, the bonnethead has a dorso-ventrally compressed anterior trunk and undulates with greater amplitude, whereas the scalloped hammerhead has a laterally compressed anterior trunk and undulates with lower amplitude. We propose that differences in cross-sectional trunk morphology account for interspecific differences in undulatory amplitude. We also found that for both species, undulatory frequency is significantly greater in the anterior body compared with all other body regions. We hypothesize that the bonnethead and scalloped hammerhead swim with a double oscillation system.

KEY WORDS: Frequency, Amplitude, Second moment of area, Swimming velocity, Cephalofoil

INTRODUCTION

Hammerhead sharks (Sphyrnidae) are characterized by a laterally expanded head (cephalofoil) that varies greatly among species (Lim et al., 2010; Thomson and Simanek, 1977). The most basal hammerhead lineage, represented by the winghead shark (*Eusphyra blochii*), possesses a cephalofoil that is proportionally the largest and measures up to 50% of their total body length (Lim et al., 2010). In comparison, the bonnethead shark (*Sphyrna tiburo*) is the most recently derived species and their cephalofoil width is 18% of total body length. Generally, as cephalofoil width increases among species, pectoral fin area decreases (Thomson and Simanek, 1977). Previous studies on hammerhead sharks have focused primarily on cephalofoil morphology and its effects on hydrodynamics and sensory efficiency; however, little is known about the morphology and function of the post-cranial body. The significant morphological variation and the close phylogenetic relationship among hammerheads make them an ideal study system to examine the effects of shape on swimming performance.

Morphological differences in the body axis and caudal fin are known to affect swimming style in sharks (Flammang, 2014; Lindsey, 1979; Long and Nipper, 1996; Webb and Keyes, 1982). Stiff-bodied species tend to displace their nearly homocercal caudal fin, whereas flexible-bodied sharks originate undulation anterior to their heterocercal tails (Donley et al., 2005; Lindsey, 1979; Long and Nipper, 1996; Webb and Keyes, 1982). Stiff-bodied swimmers also undulate using smaller lateral displacements, encounter less incurred drag, and tend to be less maneuverable than their flexible-bodied counterparts (Alexander, 2003; Webb and Keyes, 1982). A previous study shows that scalloped hammerheads have significantly smaller body stiffness and are more flexible than a non-hammerhead species (Kajiura et al., 2003); however, these comparisons have not been made among hammerheads. Given the influence of body shape on swimming, our goal was to examine the effects of morphology on undulatory kinematics in two closely related hammerhead species.

Morphological variables such as body flexural stiffness, body profile and caudal fin shape are known to affect fluid movement around the body and the shape of the vortex wakes produced during swimming (Long and Nipper, 1996; Webb and Keyes, 1982). To produce forward movement, sharks must generate an undulatory wave that reaches maximum amplitude at the caudal fin, shedding a wake of water that results in forward thrust (Alexander, 2003; Ferry and Lauder, 1996; Flammang et al., 2011; Lindsey, 1979; Webb and Keyes, 1982; Wilga and Lauder, 2002). Fishes modulate this undulatory wave by changing the frequency and amplitude of lateral displacement (Hunter and Zweifel, 1971; Long et al., 2010). Increasing frequency, specifically tail beat frequency, is correlated with increasing swimming velocity, but the relationhip between amplitude and velocity is less well understood (Lauder et al., 2016; Sfakiotakis et al., 1999). Changes in frequency and amplitude also affect Strouhal number, which describes the cyclical motion of undulatory swimming (Alexander, 2003).

Undulatory reconfiguration, or changes in body shape during a tail beat, can be observed when frequency and amplitude are

[1]Florida Atlantic University, Department of Biological Sciences, 777 Glades Rd, Boca Raton, FL 33431, USA. [2]Florida Atlantic University, Department of Ocean and Mechanical Engineering, 777 Glades Rd, Boca Raton, FL 33431, USA.

*Author for correspondence (shoffmann2014@fau.edu)

S.L.H., 0000-0003-3376-0121

Received 7 February 2017; Accepted 7 June 2017

Journal of Experimental Biology

Journal of Experimental Biology (2017) 220, 3336-3343 doi:10.1242/jeb.157941

determined along the length of the body, where the traveling wave is present during forward swimming (Long et al., 2010). The amplitude of head yaw in hammerheads increases with cephalofoil size (McComb et al., 2009), but body frequencies and amplitudes have not been documented. The goals of the present study were to: (1) quantify variations in anterior trunk morphology (fineness ratio and second moment of area); (2) compare the undulatory kinematics during volitional swimming; and (3) examine the relationship among morphological variables and swimming kinematics between two species of hammerhead shark, the bonnethead [*Sphyrna tiburo* (Linnaeus 1758)] and the scalloped hammerhead [*Sphyrna lewini* (Griffith & Smith 1834)]. Firstly, we hypothesized that anterior body morphology varied such that species with larger heads have smaller pectoral fins (Thomson and Simanek, 1977). We also predicted that bonnethead anterior trunk stiffness, as measured by second moment of area and the anterior trunk fineness ratio, is intermediate to the values previously reported for scalloped hammerheads and sandbar sharks (*Carcharhinus plumbeus*), and the anterior body fineness ratio is positively correlated with head width (Kajiura et al., 2003). Secondly, we hypothesized that the scalloped hammerhead undulates at higher amplitude than the bonnethead based on a previous study demonstrating this trend in head yaw (McComb et al., 2009). We also predicted that both species have a higher undulatory frequency in the anterior body compared with the rest of the body. Finally, we hypothesized that within each species, morphological variables correlate with swimming kinematics. We predicted that cephalofoil area is negatively correlated with anterior body amplitude, anterior body fineness ratio is positively correlated with anterior body amplitude, and pectoral fin area is negatively correlated with mid-body amplitude.

MATERIALS AND METHODS

Study animals

Volitional swimming of scalloped hammerhead sharks, *S. lewini*, was filmed at the Hawaii Institute of Marine Biology as part of an approved IACUC protocol granted to T. C. Tricas at the University of Hawaii at Manoa. Young of the year scalloped hammerhead sharks [mean total length (TL)=60.0 cm, n=4] were caught using hook and line from Kaneohe Bay, Oahu, HI, USA. Animals were housed and filmed together in a 12-foot diameter tank at the Hawaii Institute of Marine Biology after a 24 h acclimation period. Individuals of the same species were filmed together and distinguished by anatomical differences such as TL. Bonnethead sharks, *S. tiburo*, were collected in Long Key, FL, USA, and cared for under an approved IACUC protocol granted to the authors. Sub-adult to adult bonnethead sharks (mean TL=89.2 cm, n=4) were caught in shallow waters using a gill net near Long Key. Animals were housed and filmed in a 16-foot diameter tank at the Florida Atlantic University Marine Research Facility, FL, USA. Bonnetheads acclimated for 24 h prior to swimming trials and were filmed one individual at a time.

In this study, bonnethead and scalloped hammerhead sharks are in different life-history stages, but they are approximately matched for body size. Adult scalloped hammerheads mature between 140 cm TL (males) and 212 cm TL (females) and pose many captivity and husbandry challenges in a laboratory setting (Compagno, 1984). As a result of varying life history, there may be ontogenetic differences not captured in these data. We attempted to mitigate these differences by using data standardized by TL for swimming velocity and tail beat amplitudes, and size-independent variables such as flexion frequency (Hz) and flexion amplitude (deg).

Morphological measurements

For each shark, we captured still images from video footage and measured the whole dorsal body area (cm^2) using ImageJ (1.38X, National Institutes of Health, Bethesda, MD, USA). We partitioned out the cephalofoil area and total pectoral fin area, which were standardized by dorsal body area. Total planing area was calculated as the sum of the cephalofoil area and pectoral fin area and was standardized by dorsal body area. To make direct comparisons with published data, we also quantified cephalofoil width (cm) as measured from eye to eye (McComb et al., 2009; Thomson and Simanek, 1977). We measured the anterior body fineness ratio, defined as the maximum width divided by the length of the anterior trunk region from the base of the cephalofoil to the origin of the pectoral fins.

To examine cross-sectional morphology of the anterior trunk, we CT scanned a bonnethead (n=1, TL=68.83 cm) and a scalloped hammerhead (n=1, TL=51.94 cm) shark on a GE Medical Systems LightSpeed 16 CT scanner with 0.625 mm slice thickness at South Florida Radiation Oncology. Single slice images (512×512 pixels) from the scans were used to calculate the second moment of area (I), a structural predictor of stiffness, at multiple points along the body as determined by individual slices at those landmarks. I was measured at five anatomical landmarks along the total length: (A) base of the cephalofoil, (B) third gill slit, (C) anterior pelvic fin origin, (D) anterior origin of the second dorsal fin and (E) caudal peduncle. I was calculated in both the dorso-ventral [$I_y=\pi(ab^3/4)$] and lateral [$I_x=\pi(a^3b/4)$] orientations. The ratio of these measurements was used to compare cross-sectional shape between the two specimens to remove the effect of body size (Mulvany and Motta, 2013). To investigate the effect of ontogeny on anterior body shape, a cross-section at the third gill slit (region B) was dissected from fresh-frozen individuals of varied body length for the scalloped hammerhead (n=4, TL=51.9–250 cm) and the bonnethead (n=10, TL=14.6–96.5 cm). Cross-sections were scaled with a 15 cm ruler and photographed with a Nikon D3300 for ImageJ analysis and I was calculated as outlined above. A simple linear regression of I_x:I_y versus TL (cm) was used to determine whether there were differences in shape through ontogeny.

Kinematic analysis

Video was filmed from a dorsal view with a GoPro Hero3 at 30 frames s^{-1} and 1080×1920 pixels as the sharks swam volitionally. A flat port housing was used and the cameras were set to a narrow field of view to eliminate the barrel distortion of GoPro cameras. Sharks occupied less than 5% of the frame and we selected trials in which individuals were centered in the frame to avoid potential distortions at the edges of the field of view. Cameras were mounted 1 m above the water surface and water depth was approximately 1 m. Variables were standardized to animal total length or variables were size independent (units of Hz or degrees) to minimize effects of varying sizes among individuals and depth of each swim in the tank. A 30 cm ruler was placed at the bottom of the tank to provide scale for the camera. To ensure that the same trials were not analyzed twice, video was analyzed sequentially to select clips in which sharks completed at least three full tail beat cycles of straight, steady swimming.

We analyzed eight anatomical landmarks using LoggerPro 3.10.1 point tracking software (Vernier Software & Technology, Beaverton, OR, USA; Fig. 1). Anatomical landmarks included: (A) tip of the rostrum, (B) midline at the gills, (C) anterior origin of the first dorsal fin, (D) anterior origin of the second dorsal fin, (E) caudal peduncle, (F) tip of the caudal fin, (G) left posterior

Journal of Experimental Biology (2017) 220, 3336-3343 doi:10.1242/jeb.157941

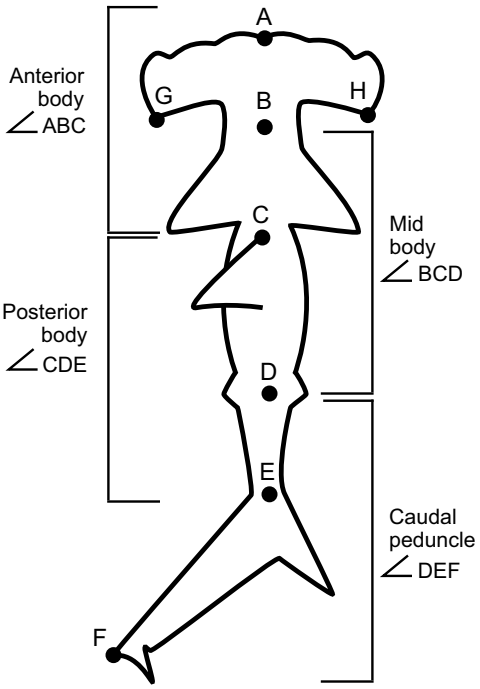

Fig. 1. Eight anatomical landmarks were digitized on each individual for both species of hammerhead shark. For regional flexion frequency and amplitude analyses, four isolated regions are outlined in brackets as the anterior body (angle ABC), mid body (angle BCD), posterior body (angle CDE) and caudal peduncle (angle DEF).

margin of the cephalofoil and (H) right posterior margin of the cephalofoil (Fig. 1). To account for noise, point tracking data were filtered using a low-pass, fourth-order Butterworth filter at 5 Hz (Erer, 2007).

We measured variables related to the overall swimming performance. We calculated velocity (V; cm s^{-1}) by measuring the displacement of point C from frame to frame over the time between frames. This was averaged over the duration of the clip (at least three tail beats). A tail beat cycle is defined as the excursion of the tail from peak lateral flexion on one side back to peak lateral flexion on the same side. We measured tail beat frequency (f; Hz) for each clip as cycles per second. Tail beat amplitude (A; cm) was measured as the peak-to-peak distance covered by the tail from full lateral flexion on one side to the full lateral flexion on the other. We then calculated Strouhal number (St) as:

$$St = \frac{Af}{V}, \quad (1)$$

where A is peak-to-peak tail beat amplitude (cm), f is tail beat frequency (Hz) and V is velocity (cm s^{-1}) (Rohr and Fish, 2004). To remove the effect of body size when comparing between species, both tail beat amplitude (A_{std}) and velocity (U; body lengths s^{-1}) were standardized by total length.

Regional flexion and amplitude were measured for the anterior body (AB) as angular displacement of the anterior trunk (point B); for the mid-body (MB) as angular displacement at the dorsal fin origin (point C); for the posterior body (PB) as angular displacement at the second dorsal fin origin (point D); and for the caudal fin (CF) as angular displacement at the caudal peduncle (point E) (Fig. 1). Flexion amplitude was measured as the maximum displaced angle from the straightened midline (180 deg) and flexion frequency was calculated as the maximum displacement per time averaged over at least three tail beats. The anterior body (AB) flexion frequency is synonymous with previously quantified head yaw (McComb et al., 2009).

Statistical analysis

For both species, video was obtained for four individuals. We selected a maximum of three clips per individual to maintain a balanced design. For each variable, we calculated the mean for each shark and we used those mean values for statistical analyses. Each variable was evaluated to ensure normality and homoscedasticity using a Shapiro–Wilk test, and variances were analyzed using ANOVA with JMP v.5.0.1.a (SAS Institute Inc., Cary, NC, USA). The flexion frequency and flexion amplitude were analyzed using mixed-effects ANOVA with species, region and the interaction term as fixed effects, and individual was coded as a random effect. *Post hoc* *t*-tests were used to compare the means of each species at each region, using a standard Bonferroni-corrected alpha value of P=0.0125. Linear regressions analyses were used to assess the relationships of kinematic variables with the morphological variables outline above.

RESULTS

Morphology

Total length (TL) and dorsal body area were significantly different between species ($F_{1,6}$=67.7894, P=0.0002 and $F_{1,6}$=53.0927, P=0.0003, respectively; Table S1). To account for size and body area differences when comparing between species, we standardized cephalofoil and pectoral fin area by dorsal body area. As predicted, standardized cephalofoil area was significantly greater in the scalloped hammerhead whereas standardized pectoral fin area was significantly higher in the bonnethead ($F_{1,6}$=51.4146, P=0.0004 and $F_{1,6}$=76.3849, P<0.0001, respectively; Fig. 2A,B). When considering the total area of the planing surface (cephalofoil area+pectoral fin area), we found that the standardized planing area was significantly greater in the scalloped hammerhead ($F_{1,6}$=18.4857, P=0.0051; Fig. 2C). Additionally, the anterior body fineness ratio was significantly higher in the scalloped hammerhead ($F_{1,6}$=63.2371, P=0.0002; Fig. 2D).

For all five regions of the body axis, I was greater in the bonnethead (Fig. 3A). To remove the effect of body size, we calculated the ratio of I measured in the dorsal-ventral direction (I_y) to that measured in the lateral direction (I_x) as a quantification of shape (Mulvany and Motta, 2013). A ratio of 1 indicates a perfect circle, greater than 1 indicates lateral body compression, and less than 1 indicates dorso-ventral body compression. For four of the five cross-sectional body regions, the scalloped hammerhead had a greater I_x:I_y ratio (Fig. 3B). Additionally, the greatest differences in cross-sectional shape between species were in the first two cross-sections at the base of the cephalofoil and third gill slit (the anterior trunk region).

To ensure the variations in anterior body cross-sectional morphology reported in Fig. 2 were not an effect of total body length (a proxy for ontogeny in each species), we examined the I_x:I_y ratio at the third gill slit among animals of varying size in the scalloped hammerhead (n=4, TL 51.9–250 cm) and the bonnethead (n=10, TL 18.5–111.5 cm; Fig. 4A). There was no significant difference in the cross-sectional shape for either species across total length; however, I_x:I_y was significantly greater in the scalloped hammerhead ($F_{1,12}$=13.4256, P=0.0032; Fig. 4B).

Kinematics

Neither velocity (m s^{-1}) nor standardized velocity (body lengths s^{-1}) was different between species (P=0.1712 and P=0.2334, respectively; Fig. 5A; Table S2). Strouhal number was not

Journal of Experimental Biology (2017) 220, 3336-3343 doi:10.1242/jeb.157941

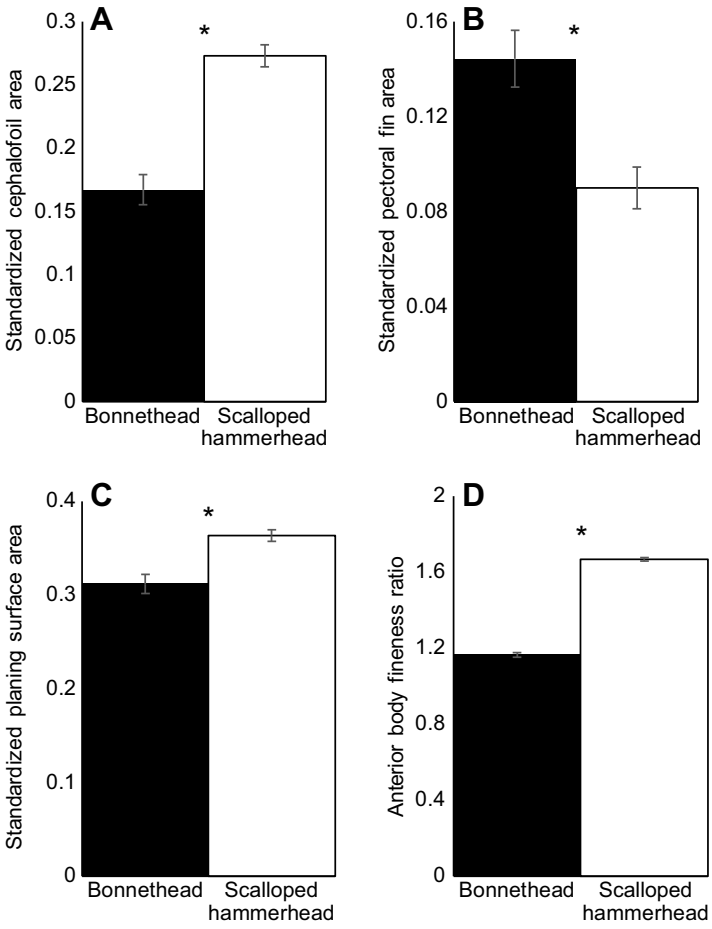

Fig. 2. Morphological differences between bonnethead (black) and scalloped hammerhead (white) bodies. (A) The cephalofoil (standardized by dorsal body area) of the scalloped hammerhead shark was 39% larger than that of the bonnethead, though the standardized pectoral fin area (B) of the bonnethead was 38% larger. (C) Standardized planing surface area (cephalofoil area+pectoral fin area) of the scalloped hammerhead was 5% greater than that of the bonnethead. (D) Anterior body fineness ratio was 30% greater in the scalloped hammerhead. Error bars represent ±s.e.m. Asterisks denote significant statistical differences (*P<0.05).

different between species (P=0.2180; Fig. 5B; Table S2). Neither tail beat frequency nor standardized tail beat amplitude differed between species (P=0.2072 and P=0.8199, respectively; Fig. 5C,D).

A mixed-effects ANOVA showed that flexion amplitude was significant with species and region as fixed effects and individual as a random effect (R^2=0.9496, P<0.0001; Fig. 6A). Flexion amplitude was significantly greater in the bonnethead with species as a fixed effect ($F_{1,6}$=9.7661, P=0.0205). Region was also a significant fixed effect ($F_{3,18}$=114.356, P<0.0001). *Post hoc* comparisons show that flexion amplitude in both species was lowest in the anterior body (AB), greatest at the caudal fin (CF), and the mid-body (MB) and posterior body (PB) were intermediate and not significantly different from one another. Between species, there was no difference in flexion amplitude in the CF; however, AB, MB and PB amplitude were significantly greater in the bonnethead (P=0.0141, P=0.0159 and P=0.0057; respectively).

Flexion frequency was also significant as a mixed-effects ANOVA with species and region as fixed effects and individual as a random effect (R^2=0.8899, P<0.0001; Fig. 6B). Region was the only significant effect ($F_{3,18}$=2.2007, P<0.0001). *Post hoc* analyses show that for both species, flexion frequency was greatest in the AB and there was no significant difference among the MB, PB and CF (P<0.0001).

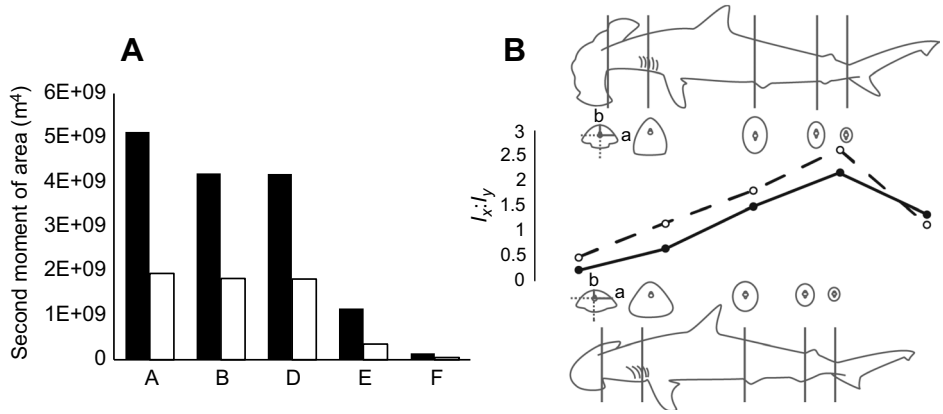

Fig. 3. Regional variation in second moment of area of the body between bonnethead (black) and scalloped hammerhead sharks (white). (A) Second moment of area (I_x) was greater in the bonnethead compared with the scalloped hammerhead at all five regions (see Fig. 1). (B) I_x:I_y was greater in the scalloped hammerhead at four of the five regions, demonstrating that the scalloped hammerhead has a more laterally compressed trunk. *a* and *b* refer to the radii used to calculate the second moment of area (I) as defined in Materials and methods, 'Morphological measurements'. The biggest differences in shape between the two species were observed in the anterior trunk region.

Journal of Experimental Biology (2017) 220, 3336-3343 doi:10.1242/jeb.157941

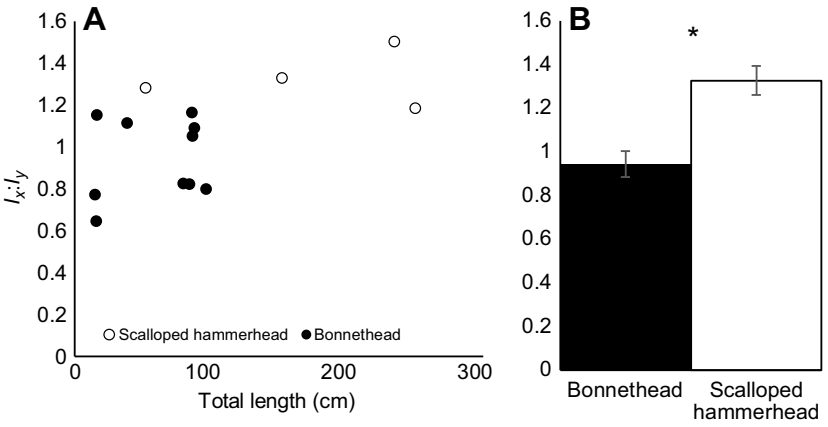

Fig. 4. Variations in anterior body cross-sectional morphology, quantified as l_x:l_y at the third gill slit. (A) There was no difference in cross-sectional shape across body sizes for either species. (B) Cross-sectional shape was approximately circular (l_x:l_y=1) in the bonnethead in comparison to the scalloped hammerhead, in which the body was laterally compressed (l_x:l_y>1). Error bars represent ±s.e.m. Asterisk denotes a significant statistical difference (*P<0.05).

We used simple linear regressions to examine the effects of morphology on flexion amplitude, which was the only kinematic variable different between species. For both species, there was no relationship between anterior body fineness ratio and anterior body amplitude, contrary to our predictions. There was also no relationship between standardized cephalofoil area and AB flexion amplitude. Finally, MB flexion amplitude was not correlated with pectoral fin area.

DISCUSSION

Previous studies have demonstrated that the closely related bonnethead (*S. tiburo*) and scalloped hammerhead (*S. lewini*) sharks differ in morphology, sensory physiology, body flexibility and head yaw amplitude (Kajiura et al., 2003; Lim et al., 2010; Mara et al., 2015; Mccomb et al., 2009; Thomson and Simanek, 1977); however, there are limited data on the effect of morphology on swimming kinematics in these two species. Our goal was to link morphological variation between species with differences in swimming kinematics. In addition to differences noted in previous studies (cephalofoil width, pectoral fin area), we showed whole-body variation in morphological variables between these species (cephalofoil area, pectoral fin area, dorsal body area, anterior fineness ratio, second moment of area; Figs 2–4). Despite having different morphologies, the swimming kinematics of these

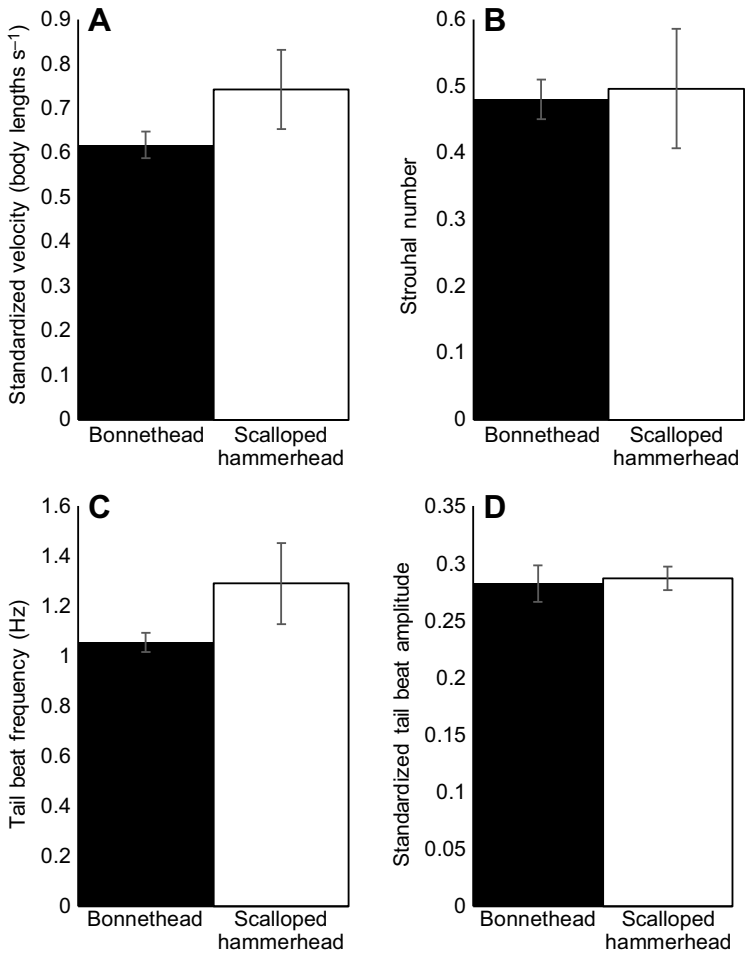

Fig. 5. Comparison of performance variables between bonnethead (black) and scalloped hammerhead (white) sharks. (A,B) Neither velocity (cm s^{-1}) nor standardized velocity (body lengths s^{-1}) was significantly different between species. (C,D) Tail beat frequency and standardized tail beat amplitude did not vary between species. Error bars represent ±s.e.m.

Journal of Experimental Biology

Journal of Experimental Biology (2017) 220, 3336-3343 doi:10.1242/jeb.157941

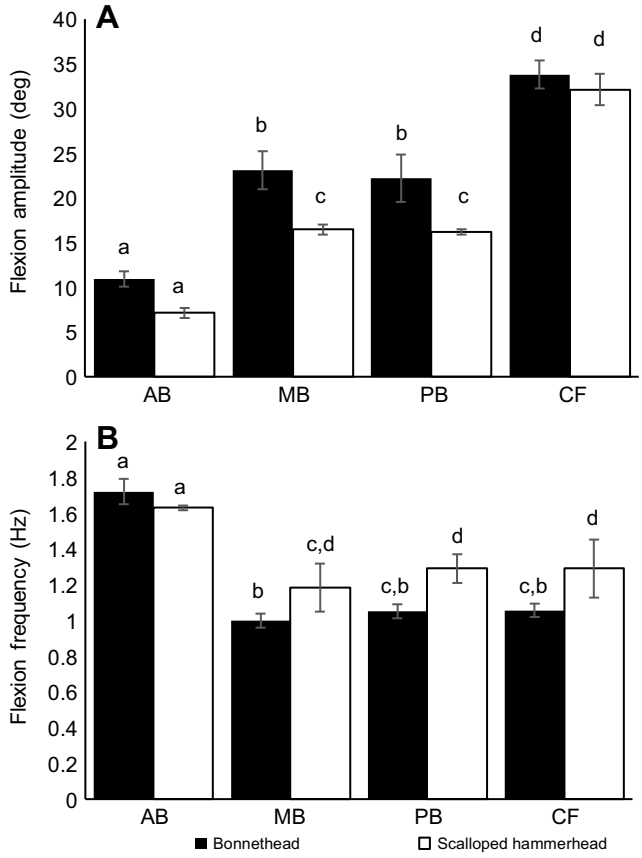

Fig. 6. Flexion variables differed between bonnethead (black) and scalloped hammerhead (white) sharks. (A) Midline amplitude increased significantly along the length of the body with the largest amplitudes produced in the caudal region. Midline amplitude differed between species at the mid-body (MB) and posterior body (PB) regions, where bonnethead amplitude was on average 28% greater than the scalloped hammerhead. (B) The anterior body (AB) had significantly higher frequencies than the three posterior regions [MB, PB and caudal fin (CF)] in both species and was not different between species. The frequency of flexion was consistent across the three posterior regions (MB, PB and CF) for both species. Error bars represent ±s.e.m. Different lowercase letters denote significant statistical differences (P<0.05).

species was similar (Fig. 5). We were not able to show any correlations among these morphological variables and kinematics within each species. However, we found that these species employ different undulatory strategies to produce similar standardized velocity (body lengths s^{-1}) and Strouhal number (Fig. 6). The scalloped hammerhead has a larger cephalofoil, narrower anterior trunk and swims at a low undulatory amplitude, whereas the bonnethead has a smaller cephalofoil, wider anterior trunk and swims at a higher amplitude.

Morphological variation

Bonnethead and scalloped hammerhead sharks show large variations in external morphology. We supported our hypothesis that the bonnethead has a proportionally smaller cephalofoil and larger pectoral fin area whereas the scalloped hammerhead had a proportionally larger cephalofoil and smaller pectoral fin area (Fig. 2). A similar inverse relationship between the cephalofoil and pectoral fin area has also been noted in the smooth hammerhead (*Sphyrna zygaena*; Thomson and Simanek, 1977). Previous data show that the inverse relationship between pectoral fin area and cephalofoil area results in the same total area of planing surfaces in the bonnethead, scalloped hammerhead and smooth hammerhead (Thomson and Simanek, 1977); however, we found that the scalloped hammerhead has a significantly larger planing surface area than the bonnethead. These data also support our hypothesis that the anterior body fineness ratio of the scalloped hammerhead shark was significantly greater than that of the bonnethead, demonstrating that the scalloped hammerhead has a narrower anterior trunk (Fig. 2D).

We predicted that the bonnethead would have an anterior trunk that is stiffer than the scalloped hammerhead but not as stiff as the sandbar shark. We found that the anterior body (AB) second moment of area (I_x) of the bonnethead is greater than that of the scalloped hammerhead, suggesting that the bonnethead anterior body is structurally stiffer (Fig. 3A) (Kajiura et al., 2003). However, the second moment of area measurements we found are greater than values previously reported for the scalloped hammerhead because of overall differences in body size, and we are unable to compare our I_x results with those reported for a non-hammerhead species (Kajiura et al., 2003). To account for the differences in body size between the bonnetheads and scalloped hammerheads in this study, we compared the cross-sectional trunk shape quantified as the ratio I_x:I_y, where values greater than 1 indicate lateral compression and values less than 1 indicate dorso-ventral compression. The greater I_x:I_y ratios at four of the five cross-sectional regions further suggest that the trunk of the scalloped hammerheads is laterally compressed and likely more flexible than the bonnethead (Fig. 3B). The bonnethead has significantly more dorso-ventrally compressed anterior trunk and is probably stiffer than the scalloped hammerhead (Fig. 3B). We also demonstrated that across ontogeny, there is no change in anterior trunk shape in both species, and the bonnethead has a significantly more dorso-ventrally compressed anterior trunk and is likely stiffer than the scalloped hammerhead (Fig. 4).

Undulatory variation

In addition to differences in trunk cross-sectional morphology and stiffness, we found that bonnethead and scalloped hammerhead sharks modulate the frequency and amplitude of the undulatory wave to produce overall similar kinematic outputs. Standardized velocity (U), Strouhal number (St), tail beat frequency (f) and standardized tail beat amplitude (A_{std}) were statistically similar between species (Fig. 5). Based on previous studies showing that the scalloped hammerhead has a greater amplitude of head yaw, we hypothesized that the scalloped hammerhead would have a greater undulatory amplitude at all body regions compared with the bonnethead. We found differences in regional flexion amplitude between species; however, as predicted, the mid-body and posterior body were significantly more displaced in the bonnethead than in the scalloped hammerhead (Fig. 6A). We suggest that differences in mid-body amplitude may be a result of differing cross-sectional trunk morphology; however, we were not able to directly test this relationship with our data, as we were unable to obtain cross-sectional data from the sharks used in the kinematic analyses.

We supported our hypothesis that the anterior body undulates at a higher frequency than the rest of the body in both species (Fig. 6B). The white sturgeon, *Acipenser transmontanus*, swims using a double oscillating system, where undulatory frequency in the anterior body differs from that in the rest of the body (Fig. 6B) (Long, 1995). These complexities in undulatory wave propagation have also been observed in the lamprey and eel, and they may stand apart from the traditional rigid-bodied teleost model, where undulatory amplitude increases rostro-caudally (Long, 1995; Root et al., 1999; Long et al., 2010). With the exception of the eel, these

patterns have been observed in fishes with cartilaginous vertebral columns or notochords, and are perhaps due to the mechanical properties of cartilaginous fishes (Porter et al., 2014, 2016; Long et al., 2002, 2004). It has been suggested that anterior body flexion may be a result of recoil from body undulation, or that it may control the driving frequency of undulation; however, recent studies show that movement of fishes' heads increases their sensitivity to external stimuli (McHenry et al., 1995; Webb, 1988, Akanyeti et al., 2016). Additionally, fish may have morphological adaptations associated with damping or selectively alter damping coefficients to minimize the effect recoil and higher order harmonics (Lighthill, 1977; Long, 1998; Root et al., 1999; Webb, 1988). We suggest that bonnethead and scalloped hammerhead sharks increase anterior body frequency independently from the rest of the body to increase sensory perception (i.e. electroreception and vision) (Kajiura and Holland, 2002; McComb et al., 2009). Increased anterior body frequency (yaw defined in McComb et al., 2009) is particularly important for the bonnethead and scalloped hammerhead because it increases the area covered by the cephalofoil when scanning for bioelectric fields, a crucial hunting behavior in benthic animals (Kajiura, 2001; Kajiura and Holland, 2002). Furthermore, head yaw increases the visual binocular overlap by upwards of 15 deg in both species (McComb et al., 2009). The greater anterior body flexion frequency for both species may allow bonnethead and scalloped hammerhead sharks to increase sensory perception without increasing whole-body frequency and the associated energetic cost (Fig. 6B). Finally, the double oscillation system shown here, in which the anterior body undulates at a different frequency than the posterior body, may be specific to cartilaginous fishes (Long, 1995). Shark vertebral columns are non-linear, viscoelastic systems that store and transmit energy, behaving as both a spring and a brake, which allows for the differential transmission of power depending on the undulatory amplitude and frequency (Porter et al., 2014, 2016). We hypothesize that the variable mechanical behavior of the cartilaginous vertebral column allows for high-frequency undulation in the anterior body without disrupting lower-frequency, posterior body undulation.

Finally, we did not support our hypothesis that morphological variables would correlate with swimming kinematics within each species. We found no relationship between cephalofoil area and anterior body amplitude, anterior body fineness ratio and anterior body amplitude, or pectoral fin area and mid-body amplitude. These results may be due to the high variability associated with volitional swimming kinematics and the narrow range of morphological variability within our individuals. Future studies may examine the relationship between morphological variables and swimming kinematics of hammerhead sharks, where differences may be evident when examining more species or a greater variation in sizes.

We show that bonnethead and scalloped hammerhead morphology varies along the length of the whole body dorsally and in cross-section (Figs 2–4). We propose that the differences in undulatory amplitude observed between these species are a result of trunk stiffness (as measured by second moment of area and anterior body fineness ratio) and cephalofoil width (Figs 2–4). We were not able to correlate any of the 2D morphological variables examined here with swimming kinematic outputs. Future studies should focus on examining the relationship between variations in second moment of area along the body with differences in flexion amplitude and frequency.

Conclusions

Previous literature has focused primarily on the morphology and function of the cephalofoil of hammerhead sharks. This is the first study to examine whole-body morphology and swimming kinematics of two hammerhead species. We found that morphologically different scalloped hammerhead and bonnethead sharks swim at similar volitional velocities and Strouhal numbers, but modulate the amplitude of undulation differently. The scalloped hammerhead has a larger cephalofoil, laterally compressed anterior trunk and undulates at a lower flexion amplitude in comparison with the bonnethead, which has a smaller cephalofoil and dorso-ventrally compressed anterior trunk. We found that both species exhibit greater flexion frequency in the anterior body, setting up a double oscillating system, which we propose may be specific to fishes with cartilaginous skeletons. We hypothesize that high-frequency head yaw increases sensory perception without the added energetic costs, increasing undulatory frequency throughout the whole body.

Acknowledgements

We thank M. E. Bowers, S. C. Leigh and the Keys Marine Laboratory for assistance in the collection and husbandry of bonnethead sharks. We thank T. C. Tricas for video of the volitional swimming of hammerhead sharks at the Hawaii Institute of Marine Biology. We thank R. Sanders and R. McConkey for assistance with digitizing video clips. We thank Mote Marine Laboratory for collecting bonnethead and scalloped hammerhead specimens for CT scanning under FWC-SAL-13-0041-SRP, and T. Leventouri, S. Pella and T. L. Meredith for CT scanning time. We thank L. J. Natanson and D. Adams for collection of fresh-frozen scalloped hammerhead and bonnethead specimens. S. M. Kajiura, P. J. Motta and J. H. Long Jr also provided thoughtful advice throughout this project and on the manuscript. This manuscript has been greatly improved owing to the comments from three anonymous reviewers.

Competing interests

The authors declare no competing or financial interests.

Author contributions

Conceptualization: S.L.H., M.E.P.; Methodology: S.L.H., S.M.W., M.E.P.; Formal analysis: S.L.H., M.E.P.; Investigation: S.L.H., S.M.W., M.E.P.; Resources: S.L.H., S.M.W., M.E.P.; Writing – original draft: S.L.H., M.E.P.; Writing – review & editing: S.L.H., M.E.P.; Supervision: S.L.H., M.E.P.; Project administration: S.L.H., M.E.P.

Funding

This research was supported by the United States National Science Foundation (IOS-649 0922605) and Florida Atlantic University startup funds to M.E.P.

Data availability

All data used are available on Dataverse: doi:10.7910/DVN/OWZA6P.

Supplementary information

Supplementary information available online at
http://jeb.biologists.org/lookup/doi/10.1242/jeb.157941.supplemental

References

Akanyeti, O., Thornycroft, P. J. M., Lauder, G. V., Yanagitsuru, Y. R., Peterson, A. N. and Liao, J. C. (2016). Fish optimize sensing and respiration during undulatory swimming. *Nat. Commun.* **7**, 11044.

Alexander, R. M. (2003). *Principles of Animal Locomotion*. Princeton, NJ: Princeton University Press.

Compagno, L. J. V. (1984). *FAO Species Catalogue, vol. 4, Sharks of the World*. Rome: Food and Agricultural Organization of the United Nations.

Donley, J. M., Shadwick, R. E., Sepulveda, C. A., Konstantinidis, P. and Gemballa, S. (2005). Patterns of red muscle strain/activation and body kinematics during steady swimming in a lamnid shark, the shortfin mako (*Isurus oxyrinchus*). *J. Exp. Biol.* **208**, 2377-2387.

Erer, K. S. (2007). Adaptive usage of the Butterworth digital filter. *J. Biomech.* **40**, 2934-2943.

Ferry, L. and Lauder, G. V. (1996). Heterocercal tail function in leopard sharks: a three-dimensional kinematic analysis of two models. *J. Exp. Biol.* **199**, 2253-2268.

Flammang, B. E. (2014). The fish tail as a derivation from axial musculoskeletal anatomy: an integrative analysis of functional morphology. *Zoology* **117**, 86-92.

Flammang, B. E., Lauder, G. V., Troolin, D. R. and Strand, T. E. (2011). Volumetric imaging of fish locomotion. *Biol. Lett.* **7**, 695-698.

Hunter, J. R. and Zweifel, J. R. (1971). Swimming speed, tail beat frequency, tail beat amplitude, and size in jack mackerel, *Trachurus symmetricus*, and other fish. *Fish. Bull.* **69**, 253-266.

Kajiura, S. M. (2001). Head morphology and electrosensory pore distribution of carcharhinid and sphyrnid sharks. *Environ. Biol. Fish.* 61, 125-133.

Journal of Experimental Biology

Kajiura, S. M. and Holland, K. N. (2002). Electroreception in juvenile scalloped hammerhead and sandbar sharks. *J. Exp. Biol.* **205**, 3609-3621.
Kajiura, S. M., Forni, J. B. and Summers, A. P. (2003). Maneuvering in juvenile carcharhinid and sphyrnid sharks: the role of the hammerhead shark cephalofoil. *Zoology* **106**, 19-28.
Lauder, G. V., Anderson, E. J., Garborg, C. S., Thornycroft, P., Turner, E., Kalionzes, K. and Kenaley, C. P. (2016). Revisiting the relationship between tail beat frequency, amplitude, and speed in swimming fishes. *Int. Comp. Biol.* **56**, E123.
Lighthill, M. J. (1977). Mathematical theories of fish swimming. In *Fisheries Mathematics* (ed. J. H. Steele), pp. 131-144. New York: Academic Press.
Lim, D. D., Motta, P., Mara, K. and Martin, A. P. (2010). Phylogeny of hammerhead sharks (Family Sphyrnidae) inferred from mitochondrial and nuclear genes. *Mol. Phylogenet. Evol.* **55**, 572-579.
Lindsey, C. C. (1979). Form, Function, and Locomotory Habits in Fish. *Fish Physiol.* **7**, 1-100.
Long, J. H. (1998). Muscles, elastic energy, and the dynamics of body stiffness in swimming eels. *Am. Zool.* **38**, 771-792.
Long, J. H.Jr. (1995). Morphology, mechanics, and locomotion: the relation between the notochord and swimming motions in sturgeon. *Environ. Biol. Fishes.* **16**, 199-211.
Long, J. H., Jr and Nipper, K. S. (1996). The importance of body stiffness in undulatory propulsion. *Am. Zool.* **36**, 678-694.
Long, J. H., Koob-Emunds, M., Sinwell, B. and Koob, T. J. (2002). The notochord of hagfish, *Myxine glutinosa*: viscoelastic properties and mechanical functions during steady swimming. *J. Exp. Biol.* **205**, 3819-3831.
Long, J. H., Koob-Emunds, M. and Koob, T. J. (2004). The mechanical consequences of vertebral centra. *Bull. Mount Desert Island Biol. Lab.* **43**, 99-101.
Long, J. H., Porter, M. E., Root, R. G. and Liew, C. W. (2010). Go reconfigure: how fish change shape as they swim and evolve. *Integr. Comp. Biol.* **50**, 1120-1139.
Mara, K. R., Motta, P. J., Martin, A. P. and Hueter, R. E. (2015). Constructional morphology within the head of hammerhead sharks (sphyrnidae). *J. Morphol.* **276**, 526-539.
Mccomb, D. M., Tricas, T. C. and Kajiura, S. M. (2009). Enhanced visual fields in hammerhead sharks. *J. Exp. Biol.* **212**, 4010-4018.
Mchenry, M., Pell, C. and John, J. H. (1995). Mechanical control of swimming speed: stiffness and axial wave form in undulating fish models. *J. Exp. Biol.* **198**, 2293-2305.
Mulvany, S. and Motta, P. J. (2013). The morphology of the cephalic lobes and anterior pectoral fins in six species of batoids. *J. Morphol.* **274**, 1070-1083.
Porter, M. E., Diaz, C., Sturm, J. J., Grotmal, S., Summers, A. P. and Long, J. H. (2014). Built for speed: strain in the cartilaginous vertebral columns of sharks. *Zoology* **117**, 19-27.
Porter, M. E., Ewoldt, R. H. and Long, J. H. (2016). Automatic control: the vertebral column of dogfish sharks behaves as a continuously variable transmission with smoothly shifting functions. *J. Exp. Biol.* **219**, 2908-2919.
Rohr, J. J. and Fish, F. E. (2004). Strouhal numbers and optimization of swimming by odontocete cetaceans. *J. Exp. Biol.* **207**, 1633-1642.
Root, R. G., Courtland, H. W., Twohig, E. J., Suter, R. B., Shepherd, W. R., Boetticher, N. C., Long, J. H., Pell, C. A. and Hobson, B. (1999). Swimming fish and fish-like models: the harmonic structure of undulatory waves suggests that fish actively tune their bodies. Proc. 11th Int. Symp. on Unmanned Untethered Submersible Technology. University of New Hampshire - Marine Systems pp. 378-388.
Sfakiotakis, M., Lane, D. M. and Davies, J. B. C. (1999). Review of fish swimming modes for aquatic locomotion. *IEEE J. Ocean. Eng.* **24**, 237-252.
Thomson, K. S. and Simanek, D. E. (1977). Body form and locomotion in sharks. *Integr. Comp. Biol.* **17**, 343-354.
Webb, P. W. (1988). “Steady” swimming kinematics of tiger musky, an esociform accelerator, and rainbow trout, a generalist cruiser. *J. Exp. Biol.* **138**, 51-69.
Webb, P. W. and Keyes, R. S. (1982). Swimming kinematics of sharks. *Fish. Bull.* **80**, 803-812.
Wilga, C. D. and Lauder, G. V. (2002). Function of the heterocercal tail in sharks: quantitative wake dynamics during steady horizontal swimming and vertical maneuvering. *J. Exp. Biol.* **205**, 2365-2374.

Table S1. Morphological measurements of bonnethead and scalloped hammerhead sharks ± standard error.

Species	*Total length (cm)	*Dorsal body area (cm^2)	*Cephalofoil width (cm)	*[1]Cephalofoil area	*[1]Pectoral fin area	[1]*Planing surface area	*Fineness ratio
Bonnethead	89.27 ± 3.11	590.41 ± 41.48	13.18 ± 0.52	0.17 ± 0.01	0.14 ± 0.003	0.31 ± 0.015	1.16 ± 0.03
Scalloped Hammerhead	59.96 ± 1.73	265.44 ± 16.39	15.23 ± 0.45	0.27 ± 0.01	0.09 ± 0.005	0.36 ± 0.01	1.66 ± 0.05

*Denote significant differences between species. [1]Due to the significant differences in total length (P = 0.0002) and dorsal body area (P = 0.0003), we standardized cephalofoil area, pectoral fin area, and planning surface area by the dorsal body area.

Table S2. Performance variables for bonnethead and scalloped hammerhead sharks ± standard error.

Species	[1]Standardized velocity (body lengths · s^{-1})	Tail Beat Frequency (Hz)	[1]Tail Beat Amplitude	Strouhal number
Bonnethead	0.646 ± 0.040	1.056 ± 0.038	0.282 ± 0.016	0.481 ± 0.010
Scalloped Hammerhead	0.716 ± 0.043	1.291 ± 0.16	0.287 ± 0.010	0.497 ± 0.006

*Denote significant differences between species.[1]Due to the significant differences in total length (P = 0.0002), we standardized velocity by total length and report in body lengths · s^{-1} and tail beat amplitude by total length leaving this a dimensionless variable.